(Fig. 3c). Treatment with vehicle or 6-OHDA did not result in the formation of inclusion bodies (Fig. 3b and d).

To examine the detailed structure and localization of inclusions, samples were examined using transmission electron microscopy. Oval aggregates with multiple concentric and filamentous structures were observed in the cytoplasm (Fig. 3e–h). In some cases, lysosomes appeared to engulf these structures (Fig. 3e and f).

To check the time course of inclusion formation, we examined brain sections at 6 h, 1 day, 2 days and 3 days after the injection. General increase of ubiquitin was observed 1 and 2 days after the injection (Fig. 4b). Ubiquitin-positive inclusion bodies were first detected 3 days after the injection of lactacystin (Fig. 4c). Samples examined prior to 3 days post-injection did not appear to contain inclusion bodies (Fig. 4a and b).

Whether such ubiquitin-positive inclusion bodies correspond to Lewy bodies that are mainly composed of α-synuclein is an important question, we immunostained sections with an anti-synuclein antibody (Spillantini *et al.* 1997). The antigen of this antibody is the amino acids 11–26 of human α-synuclein (AKEGVVAAAEKTKQGV) and these amino acids sequences are well conserved between human and medaka (AKDGVVAAAKTKGV). Pre-absorption by recombinant medaka α-synuclein abolished the signals of synuclein antibody, indicating this antibody indeed recognized medaka α-synuclein. However, at all post-injection time points examined, infrequent colocalization of synuclein was observed with ubiquitin-positive inclusion bodies (Fig. 4d–l).

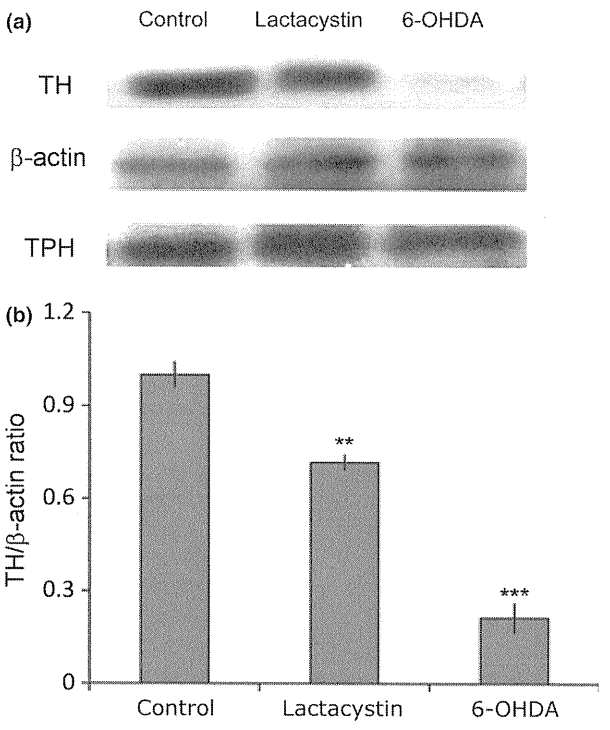

Fig. 5 Immunoblotting of TH, β-actin and tryptophan hydroxylase (TPH) in vehicle-, lactacystin- and 6-OHDA-treated medaka brain. (a) TH-specific reduction in lactacystin- and 6-OHDA-treated medaka brain. (b) Densitometric analysis of TH/β-actin band ($n = 8$). $^{**}p < 0.01$; $^{***}p < 0.001$.

Selective loss of dopaminergic and noradrenergic neurons in lactacystin-treated medaka

Immunoblotting of tryptophan hydroxylase and β-actin in lactacystin- and 6-OHDA-treated medaka brain were comparable to levels in the vehicle-treated group. However, TH signals in lactacystin- and 6-OHDA-treated medaka brain showed significant reductions, indicating specific cell loss of TH-positive neurons in these groups (Fig. 5a and b). To see whether lactacystin and 6-OHDA caused loss of dopaminergic neurons and fibers, immunohistochemistry was performed using anti-TH antibody. In medaka fish, dopaminergic neurons in the diencephalon are thought to contain an equivalent of dopaminergic neurons in human substantia nigra (Matsui *et al.* 2009). Vehicle-treated medaka showed intact TH-positive fibers in the striatum and normal TH-positive cell numbers in the diencephalon and medulla oblongata. In contrast, the TH-positive signals in the striatum decreased in lactacystin- and 6-OHDA-treated medaka (Fig. 6a–c and j). Furthermore, there was a significant decline in the number of TH-positive neurons in the middle diencephalon and locus coeruleus of lactacystin- and 6-OHDA-treated medaka brain (Fig. 6d–i, k and l). The numbers of Nissl-stained neurons in the optic tectum did not differ among vehicle-, lactacystin- and 6-OHDA-treated medaka (data not shown), indicating that the toxicity of lactacystin and 6-OHDA is specific to dopaminergic and noradrenergic neurons. The middle diencephalon and locus coeruleus were more affected than the caudal diencephalon, and the rostral diencephalon was totally spared (data not shown).

Next, we conducted TUNEL assay using the method previously described (Matsui *et al.* 2010). In the middle diencephalon of lactacystin-treated medaka brain, not in that of vehicle-treated one, TUNEL and TH double positive cells were observed (Fig. 6m–t). These findings indicated that lactacystin treatment indeed induced cell death of the TH-positive neurons in the middle diencephalon, with a fragmentation of DNA.

We used another proteasome inhibitor, epoxomicin. Epoxomicin treatment also led to inclusion body formation and similar immunohistochemical results (Fig. 7a–c). The specific vulnerability of TH-positive neurons in the middle diencephalon was also observed in epoxomicin-treated medaka (data not shown).

Finally, we measured the amount of catecholamine to confirm the effect of lactacystin and 6-OHDA on catecholamine neurons. Consistent with results from western blotting and immunohistochemistry, the amount of dopamine and

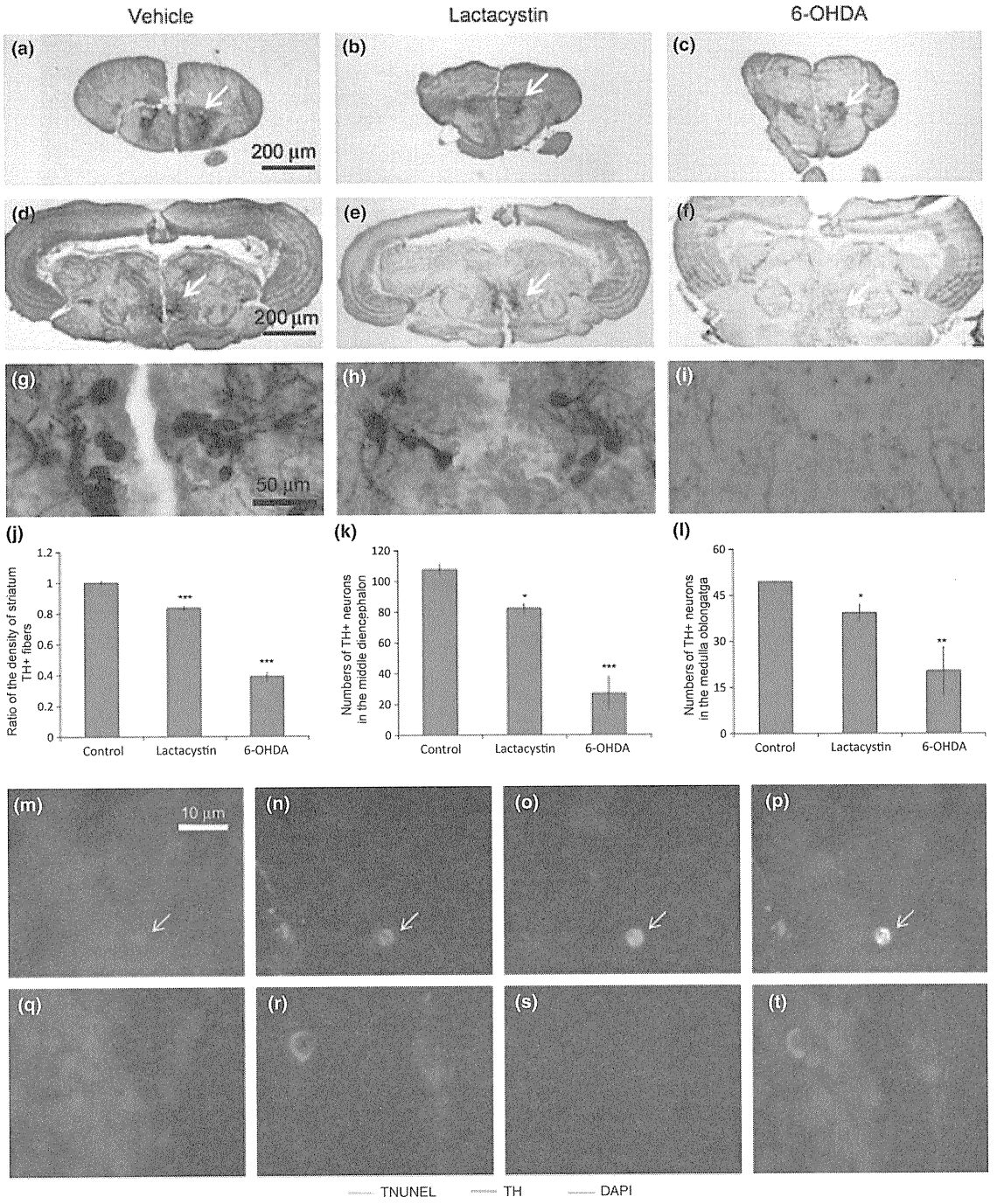

Fig. 6 TH immunohistochemistry of vehicle-, lactacystin- and 6-OHDA-treated medaka brain. (a–c) Forebrain. White arrows indicate TH-positive fibers in the striatum. (d–f) Middle diencephalon, low magnification. White arrows indicate TH-positive cell cluster. (g–i) Middle diencephalon, high magnification. (a, d, g) Vehicle-treated. (b, e, h) Lactacystin-treated. (c, f, i) 6-OHDA-treated. (j) Densitometric analysis of the striatum TH-positive fibers ($n = 4$). (k) TH-positive cell number of the middle diencephalon ($n = 8$). (l) TH-positive cell number of the locus coeruleus ($n = 8$). $^{*}p < 0.05$; $^{**}p < 0.01$; $^{***}p < 0.001$. (m–p) TUNEL and TH double-positive neurons in the middle diencephalon of lactacystin- (m–p) and vehicle- (q–t) treated medaka brain. (m, q) DAPI staining. (n, r) TH staining. (o, s) TUNEL staining. (p, t) Merged image of (m–o) and (q–s) respectively.

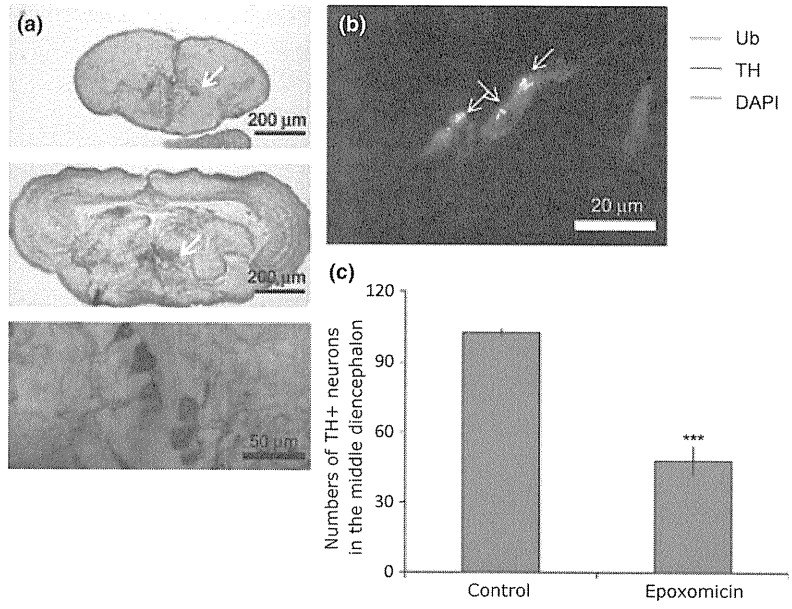

Fig. 7 Results of epoxomicin-treated medaka. (a) TH immunohistochemistry. The upper images show TH-positive fibers in the striatum (white arrow), and the middle (low magnification, white arrow indicates TH-positive cell cluster) and lower images (high magnification) show TH-positive neurons in the middle diencephalon. (b) Ubiquitin, TH-double positive neurons. White arrows indicate ubiquitin-positive inclusions. (c) The TH-positive cell number of the middle diencephalon ($n = 8$). ***$p < 0.001$.

noradrenaline decreased significantly in lactacystin- and 6-OHDA-treated medaka brain. Differences in serotonin levels between treatment groups did not reach statistical significance (Fig. 8a–c). Together with the histological findings, we concluded that proteasome inhibition as well as 6-OHDA treatment caused selective loss of dopaminergic and noradrenergic neurons in medaka brain.

Decreased spontaneous movement in lactacystin-treated medaka

Because motor disturbances are one of the definite characteristics of PD, we evaluated the swimming movements of lactacystin- and 6-OHDA-treated medaka. Spontaneous movement of lactacystin- and 6-OHDA-treated medaka gradually reduced. Three days after the injections, swimming velocity was significantly reduced in lactacystin- and 6-OHDA-treated medaka compared with vehicle-treated fish. Total swimming distance also decreased in lactacystin- and 6-OHDA-treated medaka, but the reduction in 6-OHDA-treated fish did not reach statistical significance (Fig. 9a–d).

In conclusion, proteasome inhibition in medaka brain showed similarities not only to key pathologies of PD but also to motor disturbances seen in PD patients.

Discussion

Our results demonstrate that the administration of proteasome inhibitors to medaka via the CSF induces PD-like symptoms. Fish treated with lactacystin developed inclusion bodies similar to Lewy bodies, which are associated with PD. Although proteasome inhibition in medaka brain resulted in the formation of cytoplasmic inclusion bodies throughout the CNS, the absence of inclusion bodies in 6-OHDA-injected medaka brain suggests that formation of inclusion bodies is not secondary consequence of cell death. Treatment with lactacystin also induced selective loss of dopaminergic and noradrenergic neurons and a reduction in spontaneous movement. Using identical experimental parameters, we demonstrated that specific clusters of TH-positive neurons were especially vulnerable to toxins. All of the findings seen

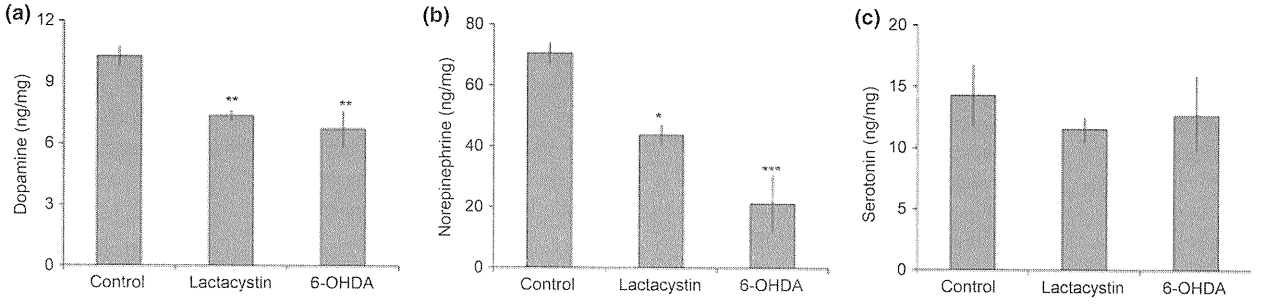

Fig. 8 HPLC analysis of catecholamine in vehicle-, lactacystin- and 6-OHDA-treated medaka brain ($n = 8$). (a) Dopamine. (b) Noradrenaline. (c) Serotonin ($n = 8$). *$p < 0.05$; **$p < 0.01$; ***$p < 0.001$.

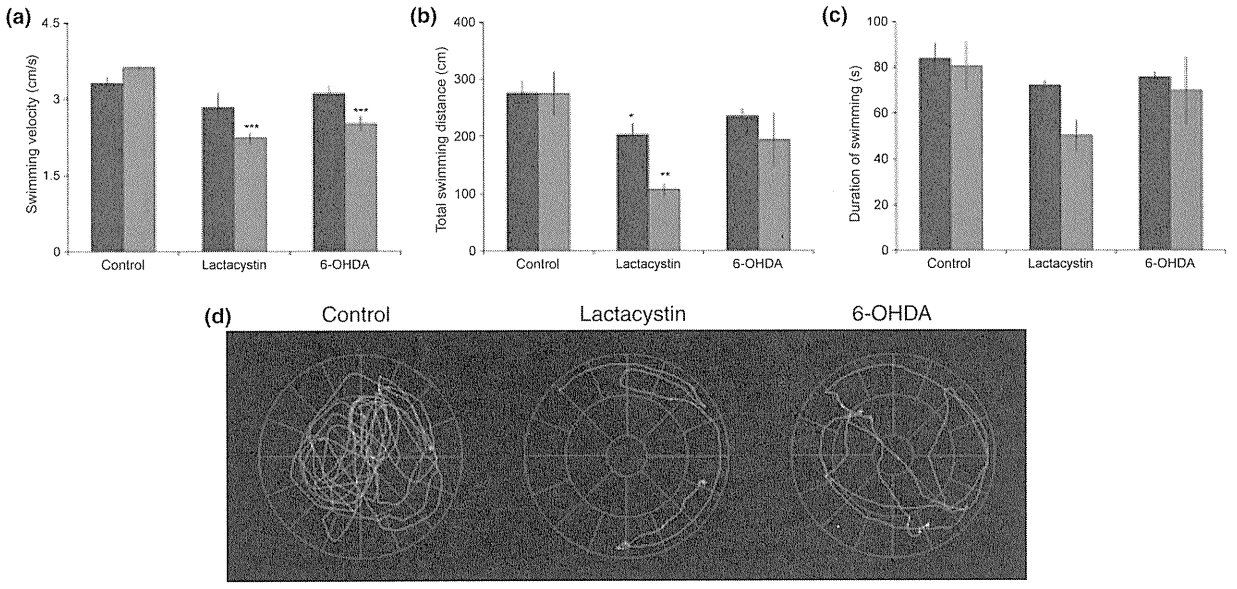

Fig. 9 Spontaneous swimming movement of vehicle-, lactacystin- and 6-OHDA-treated medaka ($n = 8$). Spontaneous swimming movement was assayed 1 (black) and 3 days (gray) after the injection. (a) Swimming velocity (cm/s). (b) Total swimming distance (cm). (c) Duration of swimming (s). (d) Representative tracks of medaka ($n = 8$). $^{*}p < 0.05$; $^{**}p < 0.01$; $^{***}p < 0.001$.

in lactacystin-treated medaka brain were also replicated by another kind of proteasome inhibitors, epoxomicin (Fig. 7a–c). This strongly suggests that the formation of inclusion bodies was indeed a result of proteasome inhibition in medaka brain.

Lactacystin, epoxomicin, 6-OHDA and MPTP (Matsui *et al.* 2009) cause selective loss of dopaminergic and noradrenergic neurons in medaka. TH-positive neurons in the middle diencephalon and locus coeruleus showed marked vulnerability to different kinds of toxins compared with other neuron clusters. The reason for this selective vulnerability is unknown, but in medaka the TH-positive neurons in the middle diencephalon and locus coeruleus have relatively large cell bodies with well-developed fibers. In rats, the nigro-striatal dopaminergic neurons also have widespread fibers (Matsuda *et al.* 2009). Large neurons may require more optimal conditions for survival and this may explain the increased vulnerability of these cells.

Because lactacystin-treated medaka demonstrated more severe deficit in the behavioral tests compared with 6-OHDA-treated medaka, there may be non-catecholaminergic effects that were not detected in our assays. Lactacystin may affect other neuronal or non-neuronal behavioral system. Further studies would be needed.

The present results are consistent with prior findings in rats demonstrating PD-like symptoms in proteasome inhibitors-treated animals (McNaught *et al.* 2004). Although the results from the earlier report have not been consistently replicated, our findings demonstrate that proteasome inhibitors are effective dopaminargic neurotoxins and may offer a good model for PD. Furthermore, the medaka is an appropriate model for testing neurochemical treatments because of the high level of accessibility to the CSF and brain. The easy accessibility of the CSF in medaka may help reduce differences in bioavailability of injected chemicals, one of the limitations of rat models.

One thing that our medaka model differed from human PD is the absence of colocalization of ubiquitin and synuclein in the inclusions. It may be due to the sensitivity of antibody we used or acute proteasome inhibition could not produce ubiquitin/synuclein double-positive inclusions. Our current aim is to replicate not only the selective loss of dopaminergic/noradrenergic neurons and movement disorders but also the formation of Lewy bodies.

Apart from the report by McNaught *et al.* and subsequent studies of proteasome inhibition in rats, this is the first study to show the loss of specific dopaminergic and noradrenergic neurons induced by the inhibition of proteasome activity. Recently, Meyer and his colleagues used the Cre-recombinase/loxP genetic approach to ablate the proteasomal Psmc1 ATPase gene and deplete 26S proteasomes in neurons in different regions of the brain to mimic neurodegeneration. Depletion of the gene in dopaminergic neurons in the substantia nigra generates a model of dopaminergic neurodedgeneration accompanied by Lewy pathology, further supporting the idea that proteasome inhibition leads to Parkinson's disease phenotype (Bedford *et al.* 2008). We believe that medaka can serve as a very useful model organism for PD research.

Acknowledgements

We wish to thank Kondoh Differentiation Signaling Project, JST, for the permission to use *Kyoto-cab* strain. We are grateful to all the people of the Department of Neurology at Kyoto University, particularly Ai Tanigaki and Rie Hikawa, who greatly supported our experiments. We are also grateful to Satoshi Fukui for excellent assistance with our electron microscopy studies.

Supporting information

Additional supporting Information may be found in the online version of this article:

Movie S1. The movie of injection procedure. Detailed information is mentioned at the Materials and methods section.

As a service to our authors and readers, this journal provides supporting information supplied by the authors. Such materials are peer-reviewed and may be re-organized for online delivery, but are not copy-edited or typeset. Technical support issues arising from supporting information (other than missing files) should be addressed to the authors.

References

Beal F. and Lang A. (2006) The proteasomal inhibiton model of Parkinson's disease: "boon or bust"? *Ann. Neurol.* **60**, 158–161.

Bedford L., Hay D., Devoy A. *et al.* (2008) Depletion of 26S proteasomes in mouse brain neurons causes neurodegeneration and Lewy-like inclusions resembling human pale bodies. *J. Neurosci.* **28**, 8189–8198.

Bové J., Zhou C., Jackson-Lewis V., Taylor J., Chu Y., Rideout H. J., Wu D. C., Kordower J. H., Petrucelli L. and Przedborski S. (2006) Proteasome inhibition and Parkinson's disease modeling. *Ann. Neurol.* **60**, 260–264.

Cook C. and Petrucelli L. (2009) A critical evaluation of the ubiquitin-proteasome system in Parkinson's disease. *Biochim. Biophys. Acta* **1792**, 664–675.

Dawson T. M. and Dawson V. L. (2003) Molecular pathways of neurodegeneration in Parkinson's disease. *Science* **302**, 819–822.

Kitada T., Asakawa S., Hattori N., Matsumine H., Yamamura Y., Minoshima S., Yokochi M., Mizuno Y. and Shimizu N. (1998) Mutations in the parkin gene cause autosomal recessive juvenile Parkinsonism. *Nature* **392**, 605–608.

Kordower J. H., Kannan N. M., Chu Y., Suresh Babu R., Stansell J., III, Terpstra B. T., Sortwell C. E., Steece-Collier K. and Collier T. J. (2006) Failure of proteasome inhibitor administration to provide a model of Parkinson's disease in rats and monkeys. *Ann. Neurol.* **60**, 264–268.

Leroy E., Boyer R., Auburger G. *et al.* (1998) The ubiquitin pathway in Parkinson's disease. *Nature* **395**, 451–452.

Manning-Boğ A. B., Reaney S. H., Chou V. P., Johnston L. C., McCormack A. L., Johnston J., Langston J. W. and Di Monte D. A. (2006) Lack of nigrostriatal pathology in a rat model of proteasome inhibition. *Ann. Neurol.* **60**, 256–260.

Matsuda W., Furuta T., Nakamura K. C., Hioki H., Fujiyama F., Arai R. and Kaneko T. (2009) Single nigrostriatal dopaminergic neurons form widely spread and highly dense axonal arborizations in the neostriatum. *J. Neurosci.* **29**, 444–453.

Matsui H., Taniguchi Y., Inoue H., Uemura K., Takeda S. and Takahashi R. (2009) A chemical neurotoxin, MPTP induces Parkinson's disease like phenotype, movement disorders and persistent loss of dopamine neurons in medaka fish. *Neurosci. Res.* **65**, 263–271.

Matsui H., Taniguchi Y., Inoue H., Kobayashi Y., Sakaki Y., Toyoda A., Uemura K., Kobayashi D., Takeda S. and Takahashi R. (2010) Loss of PINK1 in medaka fish (Oryzias latipes) causes late-onset decrease in spontaneous movement. *Neurosci. Res.* **66**, 151–161.

McNaught K. S. and Olanow C. W. (2006a) Proteasome inhibitor-induced model of Parkinson's disease. *Ann. Neurol.* **60**, 243–247.

McNaught K. S., Perl D. P., Brownell A. L. and Olanow C. W. (2004) Systemic exposure to proteasome inhibitors causes a progressive model of Parkinson's disease. *Ann. Neurol.* **56**, 149–162.

McNaught K. S., Jackson T., JnoBaptiste R., Kapustin A. and Olanow C. W. (2006b) Proteasomal dysfunction in sporadic Parkinson's disease. *Neurology* **66**, S37–S49.

Nair V. D., McNaught K. S., González-Maeso J., Sealfon S. C. and Olanow C. W. (2006) p53 mediates nontranscriptional cell death in dopaminergic cells in response to proteasome inhibition. *J. Biol. Chem.* **281**, 39550–39560.

Schapira A. H., Cleeter M. W., Muddle J. R., Workman J. M., Cooper J. M. and King R. H. (2006) Proteasomal inhibition causes loss of nigral tyrosine hydroxylase neurons. *Ann. Neurol.* **60**, 253–255.

Spillantini M. G., Schmidt M. L., Lee V. M., Trojanowski J. Q., Jakes R. and Goedert M. (1997) Alpha-synuclein in Lewy bodies. *Nature* **388**, 839–840.

Tofaris G. K., Razzaq A., Ghetti B., Lilley K. S. and Spillantini M. G. (2003) Ubiquitination of alpha-synuclein in Lewy bodies is a pathological event not associated with impairment of proteasome function. *J. Biol. Chem.* **278**, 44405–44411.

Zeng B. Y., Bukhatwa S., Hikima A., Rose S. and Jenner P. (2006) Reproducible nigral cell loss after systemic proteasomal inhibitor administration to rats. *Ann. Neurol.* **60**, 248–252.

Chemical Library Screening Identifies a Small Molecule That Downregulates SOD1 Transcription for Drugs to Treat Amyotrophic Lateral Sclerosis

GAKU MURAKAMI,[1] HARUHISA INOUE,[2,3] KAYOKO TSUKITA,[2,3] YASUYUKI ASAI,[4] YUJI AMAGAI,[5] KAZUHIRO AIBA,[5] HIROKI SHIMOGAWA,[6] MOTONARI UESUGI,[6] NORIO NAKATSUJI,[7] and RYOSUKE TAKAHASHI[1,3]

Familial amyotrophic lateral sclerosis (fALS) accounts for 10% of ALS cases, and about 25% of fALS cases are due to mutations in superoxide dismutase 1 (SOD1). Mutant SOD1-mediated ALS is caused by a gain of toxic function of the mutant protein, and the SOD1 level in nonneuronal neighbors, including astrocytes, determines the progression of ALS (non-cell-autonomous toxicity). Therefore, the authors hypothesized that small molecules that reduce SOD1 protein levels in astrocytes might slow the progression of mutant SOD1-mediated ALS. They developed and optimized a cell-based, high-throughput assay to identify low molecular weight compounds that decrease SOD1 expression transcriptionally in human astrocyte-derived cells. Screening of a chemical library of 9600 compounds with the assay identified two hit compounds that selectively and partially downregulate SOD1 expression in a dose-dependent manner, without any detectable cellular toxicity. Western blot analysis showed that one hit compound significantly decreased the level of endogenous SOD1 protein in H4 cells, with no reduction in expression of β-actin. The assay developed here provides a powerful strategy for discovering novel lead molecules for treating familial SOD1-mediated ALS. (*Journal of Biomolecular Screening* 2011;16:405-414)

Key words: amyotrophic lateral sclerosis, superoxide dismutase 1, high-throughput screening, cell-based assay

INTRODUCTION

AMYOTROPHIC LATERALS SCLEROSIS (ALS) IS A DEVASTATING neurodegenerative disease that selectively involves motor neurons in the brain and spinal cord. ALS leads to muscle weakness, paralysis, and respiratory failure within 5 years of onset. Familial ALS (fALS) accounts for about 10% of all ALS cases, and approximately 25% of fALS cases are due to mutations in superoxide dismutase [Cu-Zn] (SOD1).[1]

Some evidence suggests that mutant SOD1 protein has neurotoxic properties and leads to ALS via a gain of toxic function. Mice carrying a high copy number of the mutant SOD1 gene suffer more severe muscle weakness and death than mice carrying a low copy number.[2] SOD1 knockout mice do not develop the motor neuron disease phenotype at all.[3] In rats, only strains with the highest level of mutant SOD1 expression develop an ALS phenotype.[4]

Previous studies reported that the SOD1 level in neurons and in nonneuronal neighbors, including astrocytes and microglia, determines the onset and progression of motor neuron disease.[5,6] Therefore, we hypothesized that reduction of SOD1 expression in astrocytes might ameliorate mutant SOD1-mediated ALS. This hypothesis is supported by prolonged survival of ALS model mice, following application of RNA interference or antisense oligonucleotide, which reduced SOD1 protein levels.[7,8] Furthermore, inactivation of a mutant allele reversed the phenotypes in other neurodegenerative disease models, such as Huntington disease and Alzheimer disease, even after onset.[9,10] The present study developed and optimized a high-throughput screening (HTS) system to identify compounds that downregulate the transcription of SOD1.

MATERIALS AND METHODS

Generation of a SOD1 promotor-luciferase reporter cell line

We used the SOD1 genomic promoter, including 5′ and 3′ untranslated regions (UTR), in our construct to generate SOD1

[1]Department of Neurology, Graduate School of Medicine, Kyoto University, Kyoto, Japan.
[2]Center for iPS Cell Research and Application (CiRA), Kyoto University, Kyoto, Japan.
[3]Core Research for Evolutional Science and Technology (CREST), Japan Science and Technology Corporation, Kawaguchi, Japan.
[4]ReproCELL, Inc, Yokohama, Japan.
[5]Stem Cell and Drug Discovery Institute, Kyoto, Japan.
[6]Institute for Chemical Research, Kyoto University, Kyoto, Japan.
[7]Institute for Integrated Cell-Material Sciences, Kyoto University, Kyoto, Japan.

Received Jun 14, 2010, and in revised form Dec 7, 2010. Accepted for publication Dec 9, 2010.

Supplementary material for this article is available on the *Journal of Biomolecular Screening* Web site at http://jbx.sagepub.com/supplemental.

Journal of Biomolecular Screening 16(4); 2011
DOI: 10.1177/1087057110397888

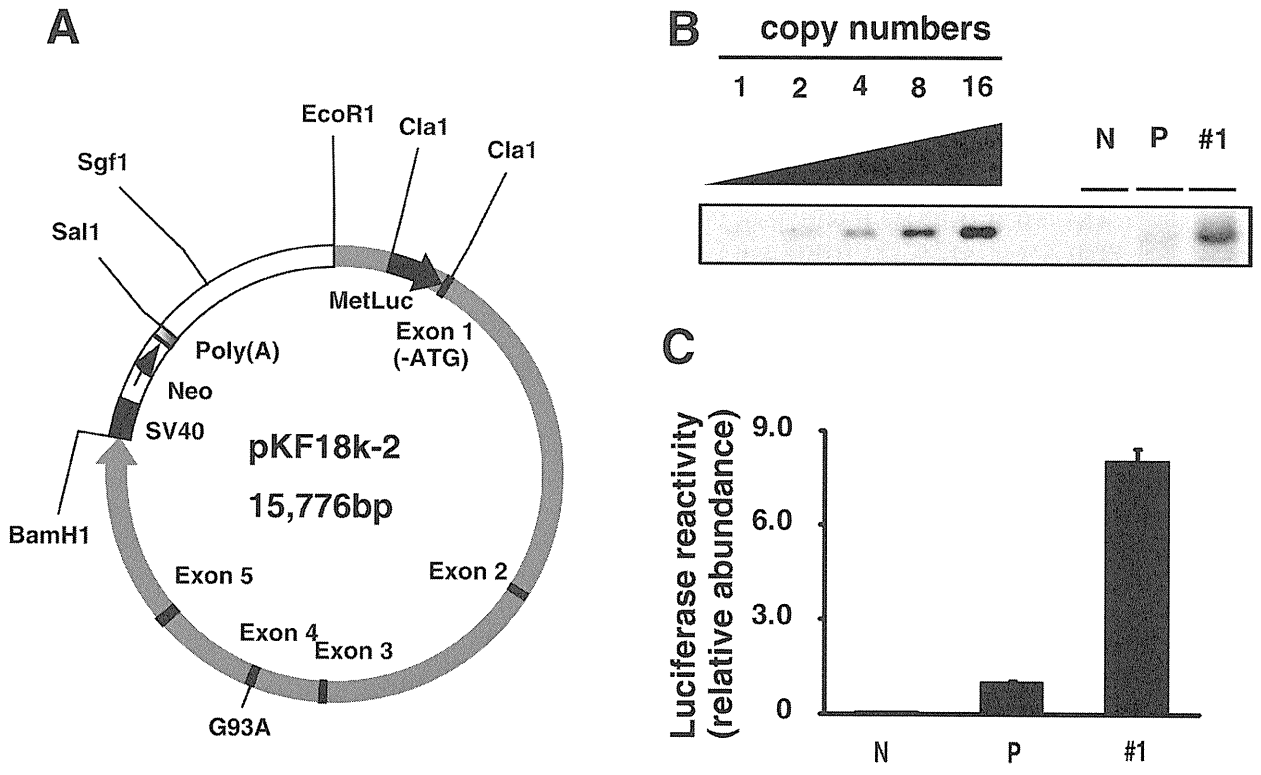

FIG. 1. The stable gPr^{SOD1}-Luc cell line used for the high-throughput screening (HTS) assay of compounds that downregulate SOD1 transcription. (**A**) Diagram of the superoxide dismutase gene (SOD1) promoter-luciferase reporter plasmid, which encodes a secreted luciferase incorporated into the human SOD1 gene, including the 5′- and 3′-untranslated region and introns. (**B**) Southern blotting analysis of the gPr^{SOD1}-Luc cell line. Clone 1 was the stable clone used in HTS assays. N, negative control, nontransfected H4 cells; P, positive control, H4 cells transiently transfected with the same cassette as clone 1. Copy number indicates the number of the transgene loaded. (**C**) Results of the luciferase reporter assay. Clone 1 has a relatively high number of copies of the transgene and, therefore, high luciferase activity. Values are mean ± SEM.

transgenic mice. The cassette was identical to that carried by SOD1^{G93A} transgenic mice (gPr^{SOD1}-Luc), to reflect physiological activity of the SOD1 promoter (**Fig. 1A**). A total of 1.2 Kb of human SOD1 (hSOD1) 5′-fragment, with 5′-EcoR1 and 3′-Afe1-BamH1 sites, was amplified using PfuUltra 2 Fusion HS DNA Polymerase (Stratagene, Cedar Creek, TX). The following PCR primers were used to amplify the region: forward primer, 5′-AAAGAATTCTGCCAACCAAATAAG-3′; reverse primer, 5′-TTTGGATCCAGCGCTGAAGCCGGAAAGCGGAG-3′. The fragment was cloned into pKF18k-2 plasmid (Takara, Otsu, Japan). To add the Cla1 site and delete the start codon of SOD1 exon 1, the cassette was amplified by PfuUltra 2 Fusion HS DNA Polymerase using the following PCR primers: forward primer, 5′-GTTATCGATGCGACGAAGGCCGTGT-3′; reverse primer, 5′-TCGCTAGGCCACGCCGAGG-3′. The fragment was cut with EcoR1 and Afe1 and cloned into pKF18k-2-hSOD1^{G93A}. The SV40-Neo-Poly(A) was incorporated downstream from the SOD1 gene, between the BamH1 and Sa11 sites. Finally, secreted luciferase gene (MetLuc) from the marine copepod, *Metridia longa* (Clontech, Mountain View, CA), with ATG was added at the Cla1 site.

Human astrocytoma-derived H4 cells,[11] which are frequently used for research on neurodegenerative diseases,[12] were used for transfection to mimic the transcription of SOD1 in astrocytes. The cell lines were cultured at 37 °C in Dulbecco's modified Eagle's medium (DMEM; Sigma, St. Louis, MO), containing 10% (v/v) fetal bovine serum (FBS), 50 U mL^{-1} penicillin, 50 μg mL^{-1} streptomycin, and 200 μg mL^{-1} G418 (Nacalai, Kyoto, Japan). The cells were stably transfected with the SOD1 genomic construct cut by Sgf1, using FuGENE 6 Transfection Reagent (Roche, Basel, Switzerland). Clonal cell lines were selected based on high levels of secreted luciferase genes, and reactivity was confirmed by Southern blotting and luciferase reporter assay (**Fig. 1B,C**). For the Southern blotting, 15 μg DNA, cut at EcoR1 and BamH1, was loaded, and the probe was made from the following primers: forward primer, 5′-ATCTGGGAGACCATGGAAGT-3′; reverse primer, 5′-TTCTTTGAAGCCGCTGATCTC-3′.

The compound library

High-throughput screening (HTS) assays using the gPr^{SOD1}-luciferase cell line were performed to screen a library of 9600

compounds provided by the Institute for Chemical Research, Kyoto University. The library was delivered in 96-well racks, with each compound dissolved in DMSO at 5 mM. The extreme right and left wells contained DMSO without any compound, leaving the corresponding well on assay plates available for controls. All compounds were stored at −20 °C.

HTS assay

Luciferase expression by the gPr^{SOD1}-luciferase cells after exposure to various small compounds was assayed in white, flat-bottomed, 96-well plates (Costar, Bethesda, MD). The cells were precultured overnight at 3.0×10^4 cells $well^{-1}$ and 37 °C. The compound to be tested was preplated, diluted with culture medium to 50 μM, and used to replace 80 μL of 100 μL per well of cell culture to give a final concentration of 40 μM. The cells were then cultured for another 16 h at 37 °C.

SOD1 gene expression by cells exposed to each compound was determined by measuring activity of luciferase proteins secreted by the cells. The cell culture in each well was transferred to the corresponding well on a 96-well assay plate, using a Multifunction Tabletop Dispenser EDR-384S2 (Biotec, Tokyo, Japan). Ready-To-Glow Secreted Luciferase Reporter System (Clontech) was added, and luciferase activity was measured as emission at 450 nm, using a 1420 VICTOR 3 Multilabel Plate Reader with optional dispenser (PerkinElmer Life and Analytical Sciences, Waltham, MA). The ratios of the vehicle-treated samples were used to correct for spontaneous decay of the signal.

Assay performance was determined by calculating the Z factor (Z′), using the following equation:

$$Z' = 1 - \frac{3 \times (\sigma_{C+} + \sigma_{C-})}{(\mu_{C-} - \mu_{C+})},$$

where μ_{C+} and σ_{C+} are the mean and standard deviation (SD), respectively, of the positive control; μ_{C-} and σ_{C-} are the mean and SD of the negative control. The positive control assays treated cells with 10 μg mL^{-1} mitomycin-C (Wako, Osaka, Japan).[13] The negative control assays treated cells with vehicle (DMSO). The Z′ value indicates the quality of an assay by describing the magnitude of the signal window ($\mu_C - \mu_{C+}$) and the precision of the assay ($\sigma_{C+} + \sigma_{C-}$). A compound was selected as a hit when it decreased luciferase activity less than mean minus 3 SD of negative controls. In each run, four or five library plates were applied to the screening assay with an individual control plate for calculating Z′ value as well as an average and SD of luciferase activity for negative control. Hits were not selected from runs with a Z′ value less than zero. The effect of hit compounds on the SOD1 expression was confirmed when it also decreased luciferase activity less than mean minus 3 SD of negative controls in duplicate by another assay.

Dose response and cytotoxicity

Dose–response analysis was carried out using the gPr^{SOD1}-luciferase cell line to confirm that the hit compounds reduced SOD1 expression in a dose-dependent manner. As in the primary assays, the cells were precultured overnight, and then the media were exchanged to give a 0- to 80-μM range of compound concentrations. The cells were incubated for another 16 h, and luciferase activity was measured. Only compounds that resulted in greater than −3 SD inhibition of SOD1 expression at 40 μM were included in further analyses because the concentration was also adapted for HTS assay selection.

Toxicity assays identified compounds that produced a nonspecific decrease in luciferase activity due to cellular toxicity. Toxicity analysis was performed on untransfected H4 cells, using the tetrazolium salt, WST-1 (Roche). In this assay, cleavage of WST-1 to formazan by mitochondrial dehydrogenases causes a color change from red to yellow. As in the primary assays, untransfected H4 cells were precultured overnight in a 96-well plate, and then the media were exchanged to give a 0- to 40-μM range of compound concentrations. The cells were incubated for 16 h, then WST-1 was added at 10 μL $well^{-1}$, and the cells were incubated for 1 h at 37 °C. Absorbance at 450 nm was compared to that of cells that were not treated with the compound. Compounds were considered to have significant cellular toxicity if cells treated with 40 μM showed greater than a −2 SD decrease in fluorescence compared to untreated cells.

Secondary assay

Enzyme-linked immunosorbent assays (ELISAs) and Western blots were used to determine whether effects observed in the reporter cell line could be reproduced at the level of endogenous SOD1 protein. As in the primary assays, untransfected H4 cells were precultured overnight, and the media were exchanged with hit compounds to give final concentrations of 0 to 40 μM. The cells were cultured for 48 h, and then each well was washed once with 200 μL of phosphate-buffered saline (PBS) and lysed with 100 μL of 1% Triton-X containing protease inhibitors (Roche).

ELISAs were performed to quantify differences in SOD1 protein levels, and EC_{50} values were calculated using a two-antibody sandwich ELISA for human SOD1. Polystyrene, enzyme-linked, immunosorbent, 96-well assay plates (Greiner Bio-one, Frickenhausen, Germany) were coated with 0.02 μg 0.1 mL^{-1} $well^{-1}$ of rabbit anti-SOD1 antibody (1:5000; cat. #SOD100; Stressgen, Ann Arbor, MI) in 50 mM sodium carbonate buffer at pH 9.4. The plates were incubated overnight at 4 °C. The wells were washed with PBS and blocked for 2 h with 3% bovine serum albumin (BSA) in wash buffer (PBS containing 0.05% Tween-20). The blocking solution was discarded; 50 μL of cell lysate diluted 1:100 in 3% BSA in wash buffer was added

to each well, along with recombinant SOD1 protein[14] (standard curve); and the plates were incubated overnight at 4 °C. The wells were washed with PBS, 100 µL of mouse anti-SOD1 antibody (1:1000; cat. #S2147; Sigma) was added, and the plates were incubated for 1 h at room temperature (RT). The wells were washed with PBS, and the bound mouse antibody was detected with 100 µL per well of horseradish peroxidase (HRP)–conjugated goat anti-mouse IgG antibody (1:5000; cat. #NA9310V; GE Healthcare, Buckinghamshire, UK). The plate was incubated for 1 h at RT and then reacted for 30 min with OptEIA TMB Substrate Reagent Set (BD Biosciences, San Jose, CA). The reaction was stopped by adding 100 µL of 1 M sodium phosphate. The rate of change in absorbance at 450 nm was measured with a ThermoFischer Scientific Multiskan JX (Thermo Electron Corporation, Waltham, MA). The concentration of SOD1 in the cell lysates was derived from a standard curve with a linear concentration range of 1.0 to 125 ng mL^{-1}.

The cell lysates were subjected to sodium dodecyl sulfate polyacrylamide gel electrophoresis (SDS-PAGE) and transferred to polyvinylidene difluoride membranes. Membranes were blocked in 3% BSA in TBS, probed with anti-SOD1 antibody (1:1000; Stressgen), and then reprobed with an anti-β-actin antibody (1:5000; cat. #A1978; Sigma) as an internal control.

Western blot analysis for phosphorylation of transcription factors

Untransfected H4 cells were precultured overnight on 12-well plates at 5.0×10^4 cells. The hit compound was diluted with culture medium to 25 µM and 50 µM and used to replace 0.8 mL of 1 mL per well of cell culture to give a final concentration of 20 µM and 40 µM, respectively. The cells were then cultured for another 16 h, and then each well was washed once with 2 mL PBS and lysed with 100 µL of 1% Triton-X containing protease inhibitors (Roche) and phosphatase inhibitor cocktail (Nacalai Tesque, Kyoto, Japan). Western blotting was performed with antibody specific to Ser^{40}-phosphorylated Nrf2 (2500:1; #EP1809Y; Abcam, Cambridge, MA), Nrf2 (500:1; H-300; #sc13032; Santa Cruz Biotechnology, Santa Cruz, CA), Ser^{133}-phosphorylated cAMP response element binding protein (CREB; 500:1; #06-519; Millipore, Billerica, MA), CREB (1000:1; #9197; Cell Signaling, Salem, MA), and β-actin (1:5000; Sigma).

Synthesis of 052C9

6-Chloro-3-formylchromone (0.20 g, 0.96 mmol) and o-phenylene diamine (0.10 g, 0.96 mmol) were dissolved in acetic acid (5 mL). The reaction mixture was stirred at 60 °C for 16 h and then diluted with an aqueous solution of $NaHCO_3$ (20 mL). The resulting precipitate was filtered and washed with water. The residue was dissolved in trifluoroacetic acid (1 mL) and then concentrated in vacuum. To the residue was added EtOAc (3 mL), and the resulting suspension was filtered to give 052C9 (72 mg, 18%) as a trifluoroacetic acid salt.

Table 1. Z′ of All the Runs

Run No.	*Z′*
1	0.69
2	0.39
3	0.35
4	0.55
5	0.60
6	0.38
7	0.42
8	0.38
9	0.37
10	−0.04
11	0.47
12	0.46
13	0.51
14	0.38
15	0.32
16	0.40
17	0.75
18	0.52
19	0.33
20	0.12
21	0.55

Table 2. Hit Compounds Identified Using the High-Throughput Screening Assay

	No. (%)
Screened compounds	9600
Total hits	325 (3.39)
Duplicate	141 (1.47)
Dose dependency	120 (1.25)
Toxic hits	5
Analysis continuing	115 (1.20)

Hits with dose dependency were defined as compounds that reduced luciferase activity in a dose-dependent manner, with a significant effect at least at 40 µM. Toxic hit compounds also decreased reporter activity in the WST-1 assay.

RESULTS

HTS assays using the gPr^{SOD1}-Luc cell line

As evidenced by the reduction in luciferase activity (**Fig. 1B,C**), the stable gPr^{SOD1}-Luc cell line expresses secreted luciferase under the control of a genomic SOD1 promoter and, therefore, is useful for identifying compounds that decrease SOD1 expression transcriptionally. The HTS assays using the gPr^{SOD1}-Luc cell line exhibited good reproducibility, with an average Z′ value of 0.39 (range, −0.23 to 0.75). Only two runs had Z′ values below zero (**Table 1**). We did not select hit compounds from these two runs. The effect of each compound was represented as the degree of inhibition of luciferase activity compared to vehicle-treated cells (**see Supplemental Figure 1**).

Using the HTS assay, duplicate assay, and dose-dependent testing, we identified 120 hit compounds that significantly inhibited SOD1 transcription (**Table 2**). We excluded the compounds with

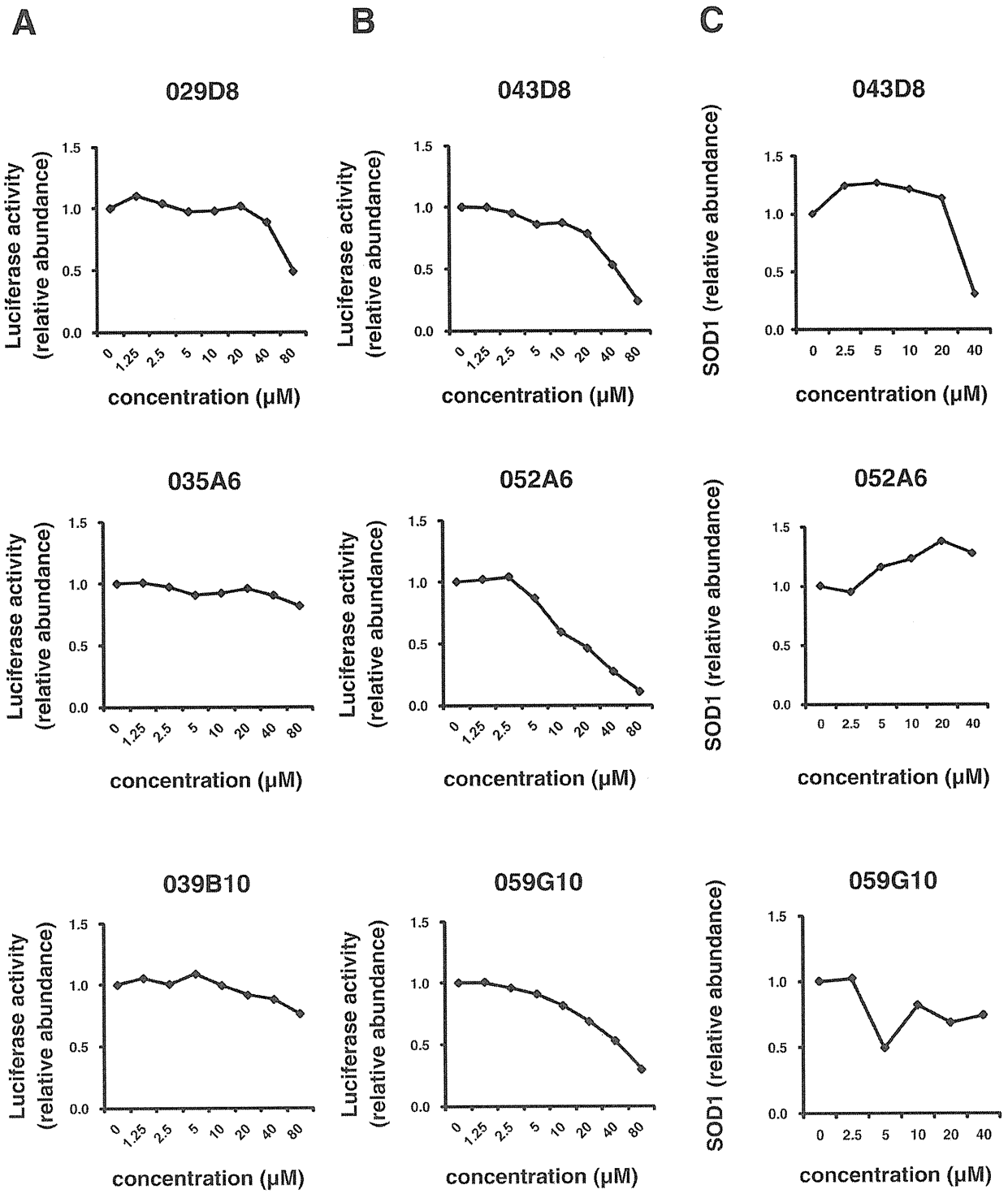

FIG. 2. (**A**) Representatives of dose-dependent effects of the excluded compounds on luciferase activity in gPr^{SOD1}-Luc cells. (**B**) Representatives of dose-dependent effects of compounds excluded by enzyme-linked immunosorbent assay (ELISA) on luciferase activity in gPr^{SOD1}-Luc cells. (**C**) Representatives of ELISA results of compounds excluded by ELISA on SOD1 abundance in H4 cells. Each point is the mean of duplicate measurements.

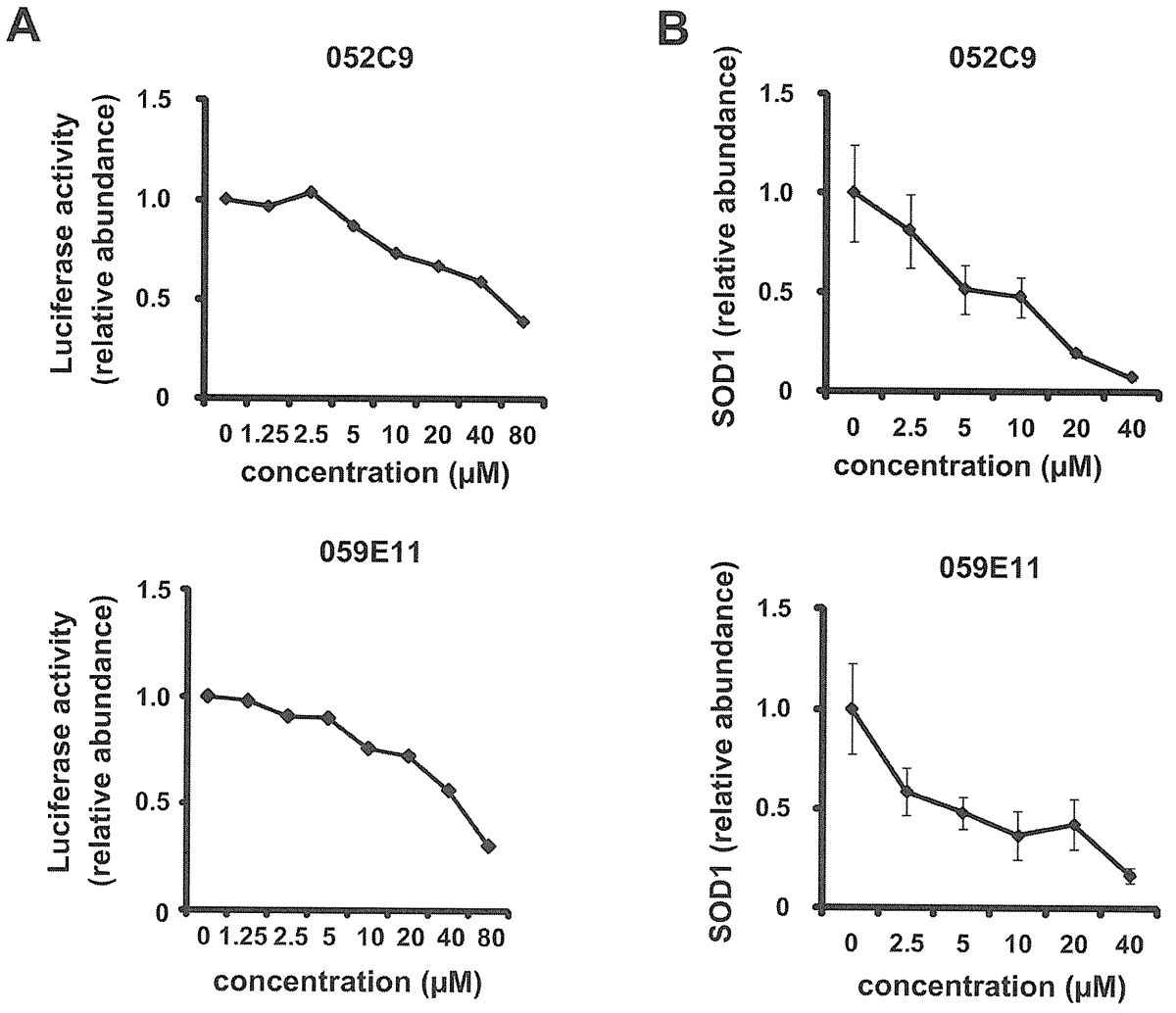

C

Hit Compounds through SOD1-ELISA

Compound	EC_{50}(μM)	TC_{50}(μM)
052C9	7.3	>40
059E11	19.6	>40

FIG. 3. (**A**) Dose-dependent effects of the hit compounds on luciferase activity in gPr^{SOD1}-Luc cells. Each point is the mean of duplicate measurements. (**B**) Enzyme-linked immunosorbent assay (ELISA) results showing effects of different concentrations of the two hit compounds on SOD1 expression. Values are means ± SEM (n = 5). (**C**) Hit compounds identified through SOD1-ELISA. EC_{50} = 50% effective concentration. TC_{50} = 50% toxic concentration.

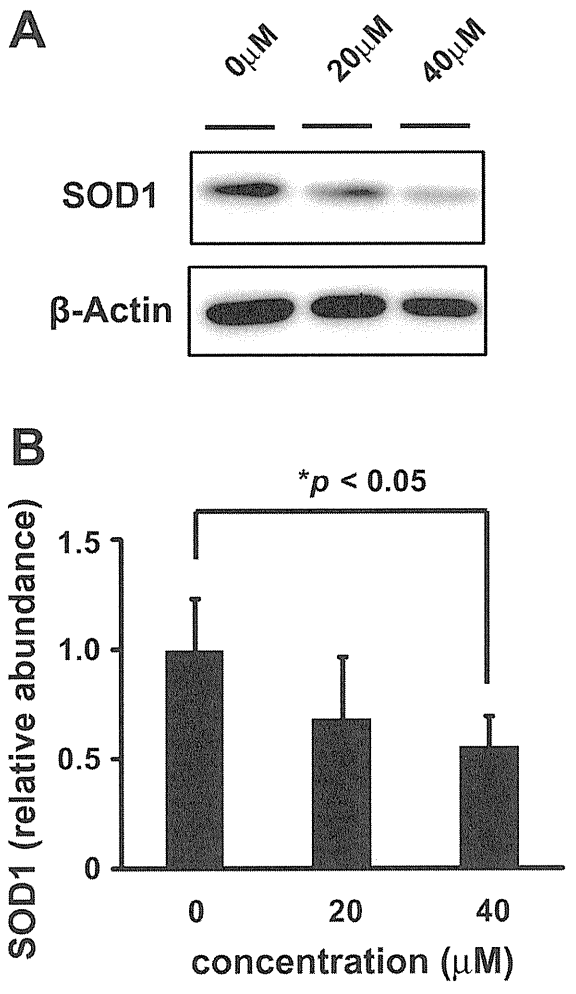

FIG. 4. (**A**) Representative Western blot showing the effect of different concentrations of the selected hit compound, 052C9, on expression of SOD1 and β-actin in H4 cells. (**B**) Band density of SOD1 relative to β-actin. Values are means ± SEM (n = 5). Difference between relative abundance at 0 and 40 μM was significant at $p < 0.05$ (one-way analysis of variance followed by the Bonferroni post hoc test).

poor dose-dependent responses (**Fig. 2A**). WST-1 assays indicated that five of these hit compounds had nonspecific cell toxicity (data not shown). ELISA results showed that 2 of the remaining 115 compounds reduced the level of endogenous SOD1 protein in a dose-dependent manner. We did not employ the compounds with no significant decline of SOD1 protein by ELISA (**Fig. 2B,C**). One of the compounds, 052C9, was selected for Western blot analysis, based on its downregulation of SOD1 expression, determined by the reporter assay (**Fig. 3A**) and by ELISA (**Fig. 3B**) with the lower 50% effective concentration (EC_{50}) compared to the other compound (**Fig. 3C**). The selected compound significantly decreased the level of endogenous SOD1 protein in H4 cells, with no reduction in expression of β-actin (**Fig. 4**). The structure of this hit compound (**Fig. 5**) was confirmed by resynthesis and spectroscopic characterization: The molecule is composed of a benzoimidazole ring and a chroman unit and is not analogous to any of the drugs used in ALS treatment trials to date. Two major transcription factors have been reported to activate the expression of SOD1: NF-E2 (Nrf2) and CREB. We examined the effects of 052C9 on the phosphorylation status of these two transcription factors by Western blot analysis. The results showed that 052C9 blocked the phosphorylation of NF-E2 (Nrf2) with no reduction of total Nrf2 protein level, whereas 052C9 had no detectable effects on the phosphorylation status of CREB (**Fig. 6**).

DISCUSSION

In a recent article, Broom et al.[15] developed HTS assays to identify compounds that downregulate SOD1 expression. On the basis of this previous study, we executed the present study targeting the transcription of SOD1 with a different compound library and a modified reporter construct of SOD1 promoter. The HTS system using astrocytoma-derived H4 cells successfully identified a number of hit compounds that decrease the expression of SOD1 protein. The HTS assays exhibited good reproducibility, with an average Z′ value of 0.39 (range, −0.23 to 0.75). This variability might be due to the manual preplating of the cells for screening or the instability of the secreted luciferase. Although the assay results had a high coefficient of variation, this could be attributed to the relatively high abundance of hit compounds (3.39%; **Table 2**). Because this hit percentage may partially reflect Gaussian statistics, we confirmed the significant efficacy of the hit compounds on SOD1 expression through another duplicate assay and dose-dependent analysis. This process would allow us to rule out the effect of Gaussian statistics on the hit selection. Although most of the hit compounds failed to decrease endogenous SOD1 protein level by ELISA in a dose-dependent manner, we suppose that this may be due to direct inhibition of luciferase reaction or to the difference between temporal patterns of the transcription and translation of SOD1. At least one of the hit compounds, 052C9, significantly downregulated SOD1 protein levels in a dose-dependent manner. It is unlikely that the effect reflects nonspecific cellular toxicity because the WST-1 assay showed no significant effects at the concentrations at which the compound exerted the downregulation of SOD1. It is also unlikely that the hit compound represses transcription generally, as there was no corresponding reduction in expression of β-actin.

The mode of action of 052C9 remains unclear at the moment. Nevertheless, our analysis suggests that 052C9 directly or indirectly blocks the phosphorylation of Nrf2. Transcription factor Nrf2 binds to the antioxidant response element (ARE) in the promoter region of detoxifying genes.[16] Phosphorylation of Nrf2 promotes its translocation into the nucleus where it activates the transcription of antioxidant genes.[17] Because the SOD1 gene also

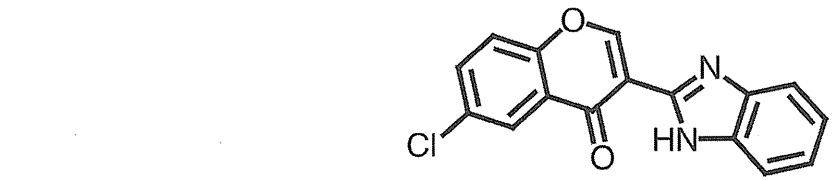

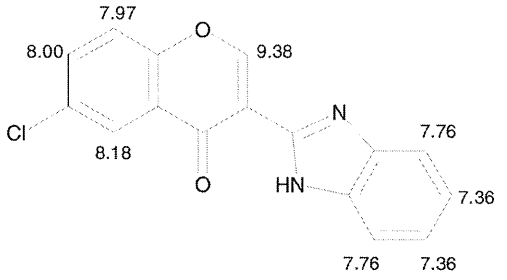

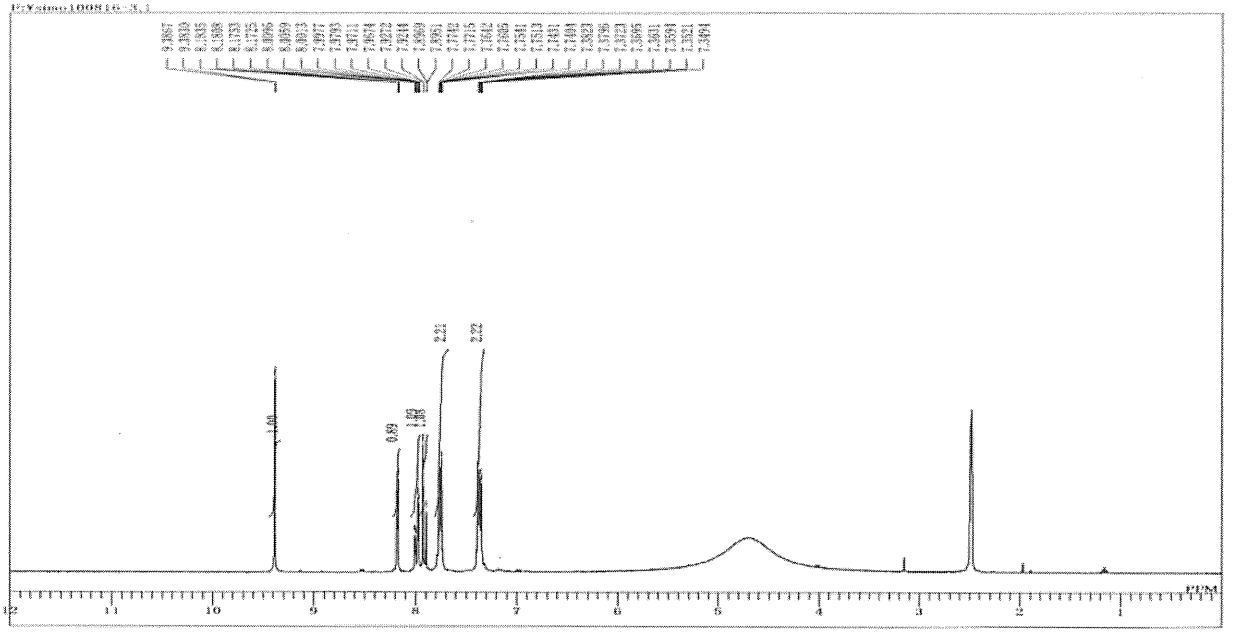

FIG. 5. The chemical structure of the selected hit compound.
^{1}H NMR (DMSO-d_6, 300 MHz) delta-$_H$ 9.38 (d, J = 1.1 Hz, 1H), 8.18 (d, J = 2.7 Hz, 1H), 7.99 (dd, J = 9.1, 2.7 Hz, 1H), 7.91 (dd, J = 9.1, 1.1 Hz, 1H), 7.76 (dd, J = 6.0, 3.0 Hz, 2H), 7.36 (dd, J = 6.0, 3.0 Hz, 2H)
^{13}C NMR (DMSO-d_6, 75 MHz) delta-$_C$ 172.9 (s), 160.0 (d), 154.1 (s), 143.5 (s), 135.2 (s), 134.4 (s × 2), 131.3 (s), 124.4 (d), 124.3 (d × 2), 124.3 (d), 121.4 (d), 114.8 (d), 111.7 (s) MS (ESI) mass calcd for $C_{16}H_9ClN_2O_2$ + H requires m/z 297 Found m/z 297

contains ARE,[18] the hit compound, 052C9, may downregulate the transcription of SOD1 by inhibiting phosphorylation of Ser^{40} of Nrf2. 052C9 had no detectable effects on the Ser^{133} phosphorylation of CREB in the present study. Because protein kinase C (PKC) phosphorylates both of the two transcription factors,[17,19] it is likely that 052C9 inhibits the activity of an unidentified Nrf2-selective kinase or its activation. 052C9 or its analogs may serve as a powerful tool for exploring the molecular mechanism of SOD1 expression.

The hit compounds identified in the present study cause a partial reduction in SOD1 expression. Although the effects on ALS-model mice have not yet been examined, partial downregulation

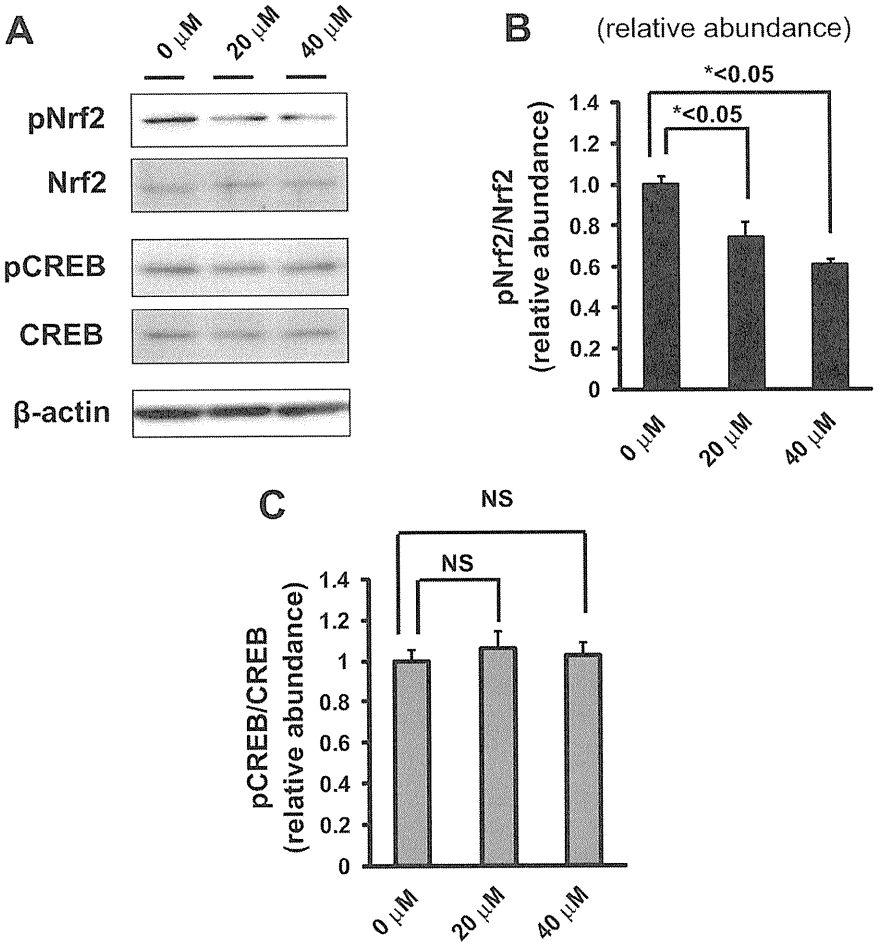

FIG. 6. (**A**) Representative Western blot showing the effect of different concentrations of the selected hit compound, 052C9, on phosphorylation of Nrf2 and cAMP response element binding protein (CREB) in H4 cells. (**B**) Band density of pNrf2 relative to Nrf2. Values are means ± SEM ($n = 7$). Differences between relative abundance both at 0 and 20 μM and at 0 and 40 μM were significant at $p < 0.05$ (one-way analysis of variance [ANOVA] followed by the Bonferroni post hoc test). (**C**) Band density of pCREB relative to CREB. Values are means ± SEM ($n = 7$). Differences between relative abundance both at 0–20 μM and at 0–40 μM were not significant (one-way ANOVA followed by the Bonferroni post hoc test).

of SOD1 expression may be desirable. SOD1-knockout mice do not develop the motor neuron disease phenotype[3] but do show modest vulnerability to axotomy[3] and pathological degeneration of neuromuscular junctions and axons.[20]

Decreasing wild-type SOD1 by a small molecule may prove to alleviate the disease phenotype in ALS-model mice and even in sporadic ALS patients. A previous study showed that wild-type (WT) SOD1 transgenic mice have pathological changes similar to those in mutant SOD1 mice and that WT SOD1 aggravates the ALS phenotype in double-transgenic mice with both WT-SOD1 and mutant SOD1.[21] Moreover, the mutation in the SOD1 promoter reduces SOD1 gene expression and may correlate with a delay in the onset of sporadic ALS.[22] Indeed, Zhong et al.[23] reported that administration of activated protein C (APC) to mutant SOD1 mice, which decreases the expression of SOD1 protein *in vivo*, ameliorates the ALS phenotype. Based on these findings, the toxicity of mutant SOD1 may not be explained by a gain of toxic function but by an increased toxicity of wild-type SOD1. Direct reduction of the transcription of pathogenic SOD1 protein may provide a new therapeutic strategy for SOD1-mediated ALS, and similar strategies may be used to treat other neurodegenerative diseases mediated by aberrant proteins.

ACKNOWLEDGMENTS

This work was supported by research grants from the Ministry of Health and Labour (R.T., H.I.), the New Energy and Industrial Technology Development Organization (NEDO)

(N.N.), JSPS (21591079) (H.I.), and JST (M.U.). We thank Ryoichi Nakano for providing the pHGSOD-Svneo plasmid and Kazumi Murai for editing the manuscript.

REFERENCES

1. Rosen, D. R.; Siddique, T.; Patterson, D.; Figlewicz, D. A.; Sapp, P.; Hentati, A.; Donaldson, D.; Goto, J.; O'Regan, J. P.; Deng, H.-X.; et al. Mutations in Cu/Zn Superoxide Dismutase Gene Are Associated with Familial Amyotrophic Lateral Sclerosis. *Nature* **1993**, *362*, 59–62.
2. Gurney, M. E.; Pu, H.; Chiu, A. Y.; Dal Canto, M. C.; Polchow, C. Y.; Alexander, D. D.; Caliendo, J.; Hentati, A.; Kwon, Y. W.; Deng, H. X.; et al. Motor Neuron Degeneration in Mice That Express a Human Cu/Zn Superoxide Dismutase Mutation. *Science* **1994**, *264*, 1772–1775.
3. Reaume, A. G.; Elliott, J. L.; Hoffman, E. K.; Kowall, N. W.; Ferrante, R. J.; Siwek, D. F.; Wilcox, H. M.; Flood, D. G.; Beal, M. F.; Brown, R. H., Jr.; et al. Motor Neurons in Cu/Zn Superoxide Dismutase-Deficient Mice Develop Normally but Exhibit Enhanced Cell Death after Axonal Injury. *Nat. Genet.* **1996**, *13*, 43–47.
4. Nagai, M.; Aoki, M.; Miyoshi, I.; Kato, M.; Pasineli, P.; Kasai, N.; Brown, R. H., Jr.; Itoyama, Y. Rats Expressing Human Cytosolic Copper-Zinc Superoxide Dismutase Transgenes with Amyotrophic Lateral Sclerosis: Associated Mutations Develop Motor Neuron Disease. *J. Neurosci.* **2001**, *21*, 9246–9254.
5. Yamanaka, K.; Chun, S. J.; Boillee, S.; Fujimoto-Tonou, N.; Yamashita, H.; Gutmann, D. H.; Takahashi, R.; Misawa, H.; Cleveland, D. W. Astrocytes as Determinants of Disease Progression in Inherited Amyotrophic Lateral Sclerosis. *Nat. Neurosci.* **2008**, *11*, 251–253.
6. Boillee, S.; Yamanaka, K.; Lobsiger, C. S.; Copeland, N. G.; Jenkins, N. A.; Kassiotis, G.; Kollias, G.; Cleveland, D. W. Onset and Progression in Inherited ALS Determined by Motor Neurons and Microglia. *Science* **2006**, *312*, 1389–1392.
7. Saito, Y.; Yokota, T.; Mitani, T.; Ito, K.; Anzai, M.; Miyagishi, M.; Taira, K.; Mizusawa, H. Transgenic Small Interfering RNA Halts Amyotrophic Lateral Sclerosis in a Mouse Model. *J. Biol. Chem.* **2005**, *280*, 42826–42830.
8. Smith, R. A.; Miller, T. M.; Yamanaka, K.; Monia, B. P.; Condon, T. P.; Hung, G.; Lobsinger, C. S.; Ward, C. M.; McAlonis-Downes, M.; Wei, H.; et al. Antisense Oligonucleotide Therapy for Neurodegenerative Disease. *J. Clin. Invest.* **2006**, *116*, 2290–2296.
9. Yamamoto, A.; Lucas, J. J.; Hen, R. Reversal of Neuropathology and Motor Dysfunction in a Conditional Model of Huntington's Disease. *Cell* **2000**, *101*, 57–66.
10. Santacruz, K.; Lewis, J.; Spires, T.; Paulson, J.; Kotilinek, L.; Ingelsson, M.; Guimaraes, A.; DeTure, M.; Ramsden, M.; McGowan, E.; et al. Tau Suppression in a Neurodegenerative Mouse Model Improves Memory Function. *Science* **2005**, *309*, 476–481.
11. Krex, D.; Mohr, B.; Hauses, M.; Ehninger, G.; Schackert, H. K.; Schackert, G. Identification of Uncommon Chromosomal Aberrations in the Neuroglioma Cell Line H4 by Spectral Karyotyping. *J. Neuro-oncol.* **2001**, *52*, 119–128.
12. Kukar, T. L.; Ladd, T. B.; Bann, M. A.; Fraering, P. C.; Narlawar, R.; Maharvi, G. M.; Healy, B.; Chapman, R.; Welzel, A. T.; Price, R. W.; et al. Substrate-Targeting c-Secretase Modulators. *Nature* **2008**, *453*, 925–930.
13. Broom, W. J.; Ay, I.; Pasinelli, P.; Brown, R. H., Jr. Inhibition of SOD1 Expression by Mitomycin C is a Non-Specific Consequence of Cellular Toxicity. *Neurosci. Lett.* **2006**, *393*, 184–188.
14. Urushitani, M.; Kurisu, J.; Tateno, M.; Hatakeyama, S.; Nakayama, K.; Kato, S.; Takahashi, R. CHIP Promotes Proteasomal Degradation of Familial ALS-Linked Mutant SOD1 by Ubiquitinating Hsp/Hsc70. *J. Neurochem.* **2004**, *90*, 231–244.
15. Broom, W. J.; Auwarter, K. E.; Ni, J.; Russel, D. E.; Yeh, L.; Maxwell, M. M.; Glicksman, M.; Kazantsev, A. G.; Brown, R. H., Jr. Two Approaches to Drug Discovery in SOD1-Mediated ALS. *J. Biomol. Screen.* **2006**, *11*, 729–735.
16. Nguyen, T.; Nioi, P.; Pickett, C. B. The Nrf2-Antioxidant Response Element Signaling Pathway and Its Activation by Oxidative Stress. *J. Biol. Chem.* **2009**, *284*, 13291–13295.
17. Huang, H. C.; Nguyen, T.; Pickett, C. B. Phosphorylation of Nrf2 at Ser40 by Protein Kinase C Regulates Antioxidant Response Element-Mediated Transcription. *J. Biol. Chem.* **2002**, *277*, 42769–42774.
18. Park, E. Y.; Rho, H. M. The Transcriptional Activation of the Human Copper/Zinc Superoxide Dismutase Gene by 2,3,7,8-Tetrachlorodibenzo-p-Dioxin through Two Different Regulator Sites, the Antioxidant Responsive Element and Xenobiotic Responsive Element. *Mol. Cell. Biochem.* **2002**, *24*, 47–55.
19. Johannessen, M.; Moens, U. Multisite Phosphorylation of cAMP Response Element-Binding Protein (CREB) by a Diversity of Protein Kinases. *Front Biosci.* **2007**, *12*, 1814–1832.
20. Flood, D. G.; Reaume, A. G.; Gruner, J. A.; Hoffman, E. K.; Hirsch, J. D.; Lin, Y.; Dorfman, K. S.; Scott, R. W. Hindlimb Motor Neurons Require Cu/Zn Superoxide Dismutase for Maintenance of Neuromuscular Junctions. *Am. J. Pathol.* **1999**, *155*, 663–672.
21. Jaarsma, D.; Haasdijk, E. D.; Grashorn, J. A. C.; Hawkins, R.; Duijn, W.; Verspaget, H. W.; London, J.; Holstege, J. C. Human Cu/Zn Superoxide Dismutase (SOD1) Overexpression in Mice Causes Mitochondrial Vacuolization, Axonal Degeneration, and Premature Motoneuron Death and Accelerates Motoneuron Disease in Mice Expressing a Familial Amyotrophic Lateral Sclerosis Mutant SOD1. *Neurobiol Dis.* **2000**, *7*, 623–643.
22. Broom, W. J.; Greenway, M.; Sadri-Vakili, G.; Russ, C.; Auwarter, K. E.; Glajch, K. E.; Dupre, N.; Swingler, R. J.; Purcell, S.; Hayward, C.; et al. 50bp Deletion in the Promoter for Superoxide Dismutase 1 (SOD1) Reduces SOD1 Expression In Vitro and May Correlate with Increased Age of Onset of Sporadic Amyotrophic Lateral Sclerosis. *Amyotroph. Lateral Scler.* **2008**, *9*, 229–237.
23. Zhong, Z.; Ilieva, H.; Hallagan, L.; Bell, R.; Singh, I.; Paquette, N.; Thiyagarajan, M.; Deane, R.; Fernandez, J. A.; Lane, S.; et al. Activated Protein C Therapy Slows ALS-Like Disease in Mice by Transcriptionally Inhibiting SOD1 in Motor Neurons and Microglia Cells. *J. Clin. Invest.* **2009**, *119*, 3437–3449.

Address correspondence to:
Haruhisa Inoue, M.D., Ph.D.
Center for iPS Cell Research and Application (CiRA)
Kyoto University 53 Shogoin Kawahara-cho,
Sakyo-ku, Kyoto, 606-8507, Japan

E-mail: haruhisa@cira.kyoto-u.ac.jp

and

Ryosuke Takahashi, M.D., Ph.D.
Department of Neurology, Graduate School of Medicine, Kyoto University
Kyoto University 54 Shogoin Kawahara-cho,
Sakyo-ku, Kyoto, 606-8507, Japan

E-mail: ryosuket@kuhp.kyoto-u.ac.jp

特集2　認知症最前線

2．疾患特異的iPS細胞を用いた神経変性疾患の研究

八幡　直樹[1,2]，井上　治久[1,2]

抄録：数種類の初期化遺伝子を体細胞に導入することにより，胚性幹細胞（embryonic stem cells：ES細胞）に匹敵する多分化能を有する人工多能性幹細胞（induced pluripotent stem cells：iPS細胞）が誕生した。神経変性疾患研究においては，これまで生体から入手が困難であった疾患の標的細胞をiPS細胞から作製することが可能になり，病態解明，創薬開発が進展すると期待されている。本稿では疾患特異的iPS細胞を用いた神経変性疾患研究と今後の展望について述べる。

日本生物学的精神医学会誌 21（4）：257−260, 2010

Key words：iPS cell, Neurodegenerative disease, drug discovery, disease modelling

1．はじめに

2006年，マウス線維芽細胞にレトロウイルスを用いて4つの初期化遺伝子（Oct3/4，Sox2，Klf4，c-Myc）を導入することによりES細胞に匹敵する多分化能を有する細胞を樹立できることが報告された[16]。この細胞は，人工多能性幹細胞（iPS細胞）と命名された。2007年，ヒトにおいても同様に，線維芽細胞からiPS細胞が樹立された[17]。iPS細胞作製技術によって，体細胞を初期化することにより疾患を有する患者さん自身の体細胞から，疾患特異的iPS細胞を経て，疾患の標的細胞を作り出すことが可能になった。特に，ES細胞の倫理的課題や拒絶反応を回避できるため，再生医療の分野にさらなる進展をもたらす可能性がある。神経変性疾患においては，生検により標的細胞を採取することは難しく，また，剖検組織は死後変化等の影響を排除しにくい。神経変性疾特異的iPS細胞を分化誘導することで，疾患標的細胞が作製可能になる。

近年，いくつかの神経変性疾患では，神経細胞自体が抱える要因だけではなく，周囲に存在するグリア細胞が神経変性に関与していることが明らかになっている[2,18]。iPS細胞作製技術を用いることで，神経細胞以外の細胞にも焦点を当てた複合的なアプローチが展開できる可能性がある。本稿では，神経変性疾患におけるiPS細胞研究の現状を概説し，病態解明，創薬開発へ向けての今後の展望を述べる。

2．神経変性疾患特異的iPS細胞研究の現状

2008年，ハーバード大学のグループらが，筋萎縮性側索硬化症（Amyotrophic lateral screlosis; ALS）の原因遺伝子の一つであるsuperoxide dismutase 1（SOD1）の変異を有する患者の皮膚線維芽細胞を用いて，iPS細胞を樹立し，motor neuron and pancreas homeobox 1（HB9）を発現する脊髄運動神経へ分化誘導を行った[4]。同年，パーキンソン病等，多種の疾患特異的iPS細胞作製の報告がある[11]。2009年に，MITのグループらが，初期化遺伝子のゲノムへの挿入がない，パーキンソン病由来iPS細胞を作製し，これらのiPS細胞をtyrosine hydroxylase（TH）陽性ドーパミン作動性神経細胞へ分化誘導を行った[14]。

2009年，survival of motor neuron 1（SMN1）遺伝子の異常による脊髄性筋萎縮症（Spinal muscular atrophy：SMA）について，疾患特異的iPS細胞を利用し，病態再現が示された[5]。SMA患者のiPS細胞を脊髄運動神経に分化誘導すると，6週間後に数および大きさの低下がみられた。また，

Neurodegenerative disease-specific induced pluripotent stem cell research

1）京都大学 iPS細胞研究所臨床応用研究部門（〒606-8507 京都市左京区聖護院川原町53）Naoki Yahata, Haruhisa Inoue：Center for iPS Cell Research and Application（CiRA），Department of Clinical application, Kyoto University, 53 Kawahara-cho, Shogoin, Sakyo-ku, Kyoto 606-8507, Japan.

2）戦略的創造研究推進事業（CREST），独立行政法人科学技術振興機構（JST）（〒332-0012 埼玉県川口市本町4-1-8）CREST, JST, 4-1-8 Honcho, Kawaguchi, Saitama 332-0012, Japan.

【井上　治久　E-mail：haruhisa@cirakyoto-u.ac.jp】

SMA患者で発現が低下しているSMNの発現を上昇させる薬剤としてしられる，バルプロ酸やトブラマイシンを投与することにより，SMNの発現が上昇し，正常レベルに近づくことが示された。同年，家族性自律神経失調症（Familial dysautonomia：FD）患者由来iPS細胞を用いた病態再現の報告がなされた[7]。この疾患は末梢神経障害を呈し，IKB kinase complex-associated protein（IKBKAP）遺伝子変異によって引き起こされる。FD患者由来iPS細胞から分化した細胞においてIKBKAPのスプライス異常産物の上昇がみられた。また，FD患者由来iPS細胞を神経堤細胞に分化誘導したところ，achaete-scute complex homolog 1（ASCL1）およびβ-Ⅲ-tubulin（Tuj1）陽性の末梢神経の数の低下や，スクラッチアッセイという方法での細胞移動の異常が観察された。さらに，IKBKAPのスプライス異常産物を減少させるとして知られるカイネチンをiPS細胞培養時に4週間処理することにより，スプライシング異常が改善した。これらの報告は，疾患特異的iPS細胞から分化誘導した細胞を使って，病態再現が可能であることと，分子生物学・生化学的解析により評価可能であることを示している。さらには，疾患特異的iPS細胞が創薬開発のためのスクリーニングに利用可能であることを示している。

3．神経変性疾患特異的iPS細胞を用いた創薬開発

ヒトで効果のある神経変性疾患治療の薬剤を開発するために，ヒトのiPS細胞から分化誘導した標的細胞が薬剤のスクリーニングに使用可能である。このスクリーニング系を構築する際に，標的となる神経細胞やグリア細胞を純度高く，大量に準備することが重要である。これを実現するためには，目的の細胞を効率よく分化誘導する技術に加え，その細胞を純化する技術が必要になる。方法としては，目的の細胞で特異的に発現する遺伝子のプロモーター制御下に蛍光タンパク質を発現するベクターを導入した細胞，あるいは目的細胞特異的な表面抗原を認識する抗体で標識をした細胞をフローサイトメトリーで回収する方法等が行われている[12]。細胞純化技術は細胞移植を行う際にも必須になると考える。疾患特異的iPS細胞を用いた創薬開発への応用には，さらに効率のよい分化誘導・純化法が重要になるであろう。

4．今後の展望

神経系への分化誘導法は，マウスES細胞の系で確立された方法を基礎に，ヒトES細胞を用いて改変がなされている。脊髄運動神経や，ドーパミン作動性神経の分化誘導法は既にいくつかのグループから報告があり[6,15]，上述の運動神経疾患やパーキンソン病の研究に用いられている。しかし，現在まで確立されている脊髄運動神経，ドーパミン作動性神経を含むさまざまな神経への分化誘導法は分化効率や時間などの観点からさらなる効率化の余地がある。ヒトES/iPS細胞からの神経堤細胞[8]，網膜細胞[10]等への分化誘導法についても既に報告がある。最近，マウスのES細胞より小脳プルキンエ細胞への効率的な分化誘導法について報告がなされ，脊髄小脳変性症の病態解明や治療法開発に向けて，ヒトiPS細胞からの誘導法への応用が期待されている[9]。

これまでiPS細胞作製技術を利用して疾患再現が行われた疾患[1,3,5,7,13]は，ほとんどが発生過程の異常がその病態に反映される疾患である。一方で，アルツハイマー病やパーキンソン病などの晩発性神経変性疾患の場合，加齢が危険因子の一つであり，発生過程における異常の有無は不明である。さらに，神経細胞に分化誘導し，成熟化した後に初めて何らかの異常や，疾患由来でない細胞との違いが観察される可能性がある。加齢変化を *in vitro* で再現するために長期の培養や，さらには加齢を加速する培養条件の検討が必要かもしれない。

神経変性疾患において原因遺伝子が同定されたものは，動物モデルや細胞モデルを用いて病態解明が進んでいる。一方，孤発性神経変性疾患の多くは，その病因が依然として不明である。iPS細胞作製技術を用いて，孤発性疾患についても患者由来の標的細胞が手に入ることから，病態解明に新たなアプローチが加わったと考えられる。孤発性神経変性疾患由来iPS細胞から分化誘導した神経細胞について，生化学的・細胞生物学的異常を解析することができれば，創薬開発の分子標的の発見につながるかもしれない。一方，家族性神経変性疾患由来iPS細胞を用いた病態再現を基準に，同じ系で孤発性神経変性疾患由来iPS細胞を用いて病態が再現できれば，診断法開発に寄与する可能性がある。

5．おわりに

本稿では，iPS細胞を用いた神経変性疾患研究について述べた。iPS細胞技術という革新的技術を用

いることによって，神経変性疾患の病態解明および創薬開発が加速することが期待される。

6．謝　辞

認知症の共同研究者である筑波大学の朝田隆先生，長崎大学の岩田修永先生，理化学研究所の西道隆臣先生，放射線医学総合研究所の須原哲也先生，樋口真人先生，神戸大学の戸田達史先生，小林千浩先生，徳島大学の和泉唯信先生，山形大学の川勝忍先生に深謝申し上げます。

文　献

1）Agarwal S, Loh YH, McLoughlin EM, et al (2010) Telomere elongation in induced pluripotent stem cells from dyskeratosis congenita patients. Nature. 464 (7286) : 292-296.
2）Boillée S, Yamanaka K, Lobsiger CS, et al (2006) Onset and progression in inherited ALS determined by motor neurons and microglia. Science, 312 (5778) : 1389-1392.
3）Carvajal-Vergara X, Sevilla A, et al (2010) Patient-specific induced pluripotent stem-cell-derived models of LEOPARD syndrome. Nature, 465 (7299) : 808-812.
4）Dimos JT, Rodolfa KT, Niakan KK, et al (2008) Induced pluripotent stem cells generated from patients with ALS can be differentiated into motor neurons. Science, 321 (5893) : 1218-1221.
5）Ebert AD, Yu J, Rose FF Jr, et al (2009) Induced pluripotent stem cells from a spinal muscular atrophy patient. Nature, 457 (7227) : 277-280.
6）Hu BY and Zhang SC (2009) Differentiation of spinal motor neurons from pluripotent human stem cells. Nat Protoc, 4 (9) : 1295-1304.
7）Lee G, Papapetrou EP, Kim H, et al (2009) Modelling pathogenesis and treatment of familial dysautonomia using patient-specific iPSCs. Nature, 461 (7262) : 402-406.
8）Lee G, Chambers SM, Tomishima MJ, et al (2010) Derivation of neural crest cells from human pluripotent stem cells. Nat Protoc, 5 (4) : 688-701.
9）Muguruma K, Nishiyama A, Ono Y, et al (2010) Ontogeny-recapitulating generation and tissue integration of ES cell-derived Purkinje cells. Nat Neurosci, 13 (10) : 1171-1180.
10）Osakada F, Jin ZB, Hirami Y, et al (2009) In vitro differentiation of retinal cells from human pluripotent stem cells by small-molecule induction. J Cell Sci, 122 (Pt 17) : 3169-3179.
11）Park IH, Arora N, Huo H, et al (2008) Disease-specific induced pluripotent stem cells. Cell, 134 (5) : 877-886.
12）Pruszak J, Sonntag KC, Aung MH, et al (2007) Markers and methods for cell sorting of human embryonic stem cell-derived neural cell populations. Stem Cells, 25 (9) : 2257-2268.
13）Raya A, Rodríguez-Pizà I, Guenechea G, et al (2009) Disease-corrected haematopoietic progenitors from Fanconi anaemia induced pluripotent stem cells. Nature, 460 (7251) : 53-59.
14）Soldner F, Hockemeyer D, Beard C, et al (2009) Parkinson's disease patient-derived induced pluripotent stem cells free of viral reprogramming factors. Cell, 136 (5) : 964-977.
15）Sonntag KC, Pruszak J, Yoshizaki T, et al (2007) Enhanced yield of neuroepithelial precursors and midbrain-like dopaminergic neurons from human embryonic stem cells using the bone morphogenic protein antagonist noggin. Stem Cells, 25 (2) : 411-418.
16）Takahashi K and Yamanaka S (2006) Induction of pluripotent stem cells from mouse embryonic and adult fibroblast cultures by defined factors. Cell, 126 (4) : 663-676.
17）Takahashi K, Tanabe K, Ohnuki M, et al (2007) Induction of pluripotent stem cells from adult human fibroblasts by defined factors. Cell, 131 (5) : 861-872.
18）Yamanaka K, Chun SJ, Boillee S, et al (2008) Astrocytes as determinants of disease progression in inherited amyotrophic lateral sclerosis. Nat Neurosci, 11 (3) : 251-253.

■ ABSTRACT

Neurodegenerative disease-specific induced pluripotent stem cell research

Naoki Yahata, Haruhisa Inoue

Center for iPS Cell Research and Application, Kyoto University

Induced pluripotent stem (iPS) cell technology shows great potential for the study of pathogenesis, and drug discovery toward neurodegenerative diseases. This review summarizes the current status on the neurodegenerative disease-specific iPS cell research and describes its potential.

(Japanese Journal of Biological Psychiatry 21 (4) : 257-260, 2010)

特集1

神経系におけるiPS細胞
iPS細胞の活用も含めた神経機能修復の現状と将来

iPS細胞技術の神経疾患研究での有用性および今後の課題

北岡志保（きたおかしほ），井上治久（いのうえはるひさ）
京都大学iPS細胞研究所臨床応用研究部門（〒606-8507 京都市左京区聖護院川原町53）
戦略的創造研究推進事業（CREST），独立行政法人科学技術振興機構（JST）
（〒332-0012 埼玉県川口市本町4-1-8）
E-mail : haruhisa@cira.kyoto-u.ac.jp

SUMMARY

iPS細胞作製技術の開発により，これまで生体から入手困難であった患者由来組織の細胞を研究材料として使用できるようになった．その結果，神経疾患特異的iPS細胞から疾患の標的細胞である神経細胞あるいはグリア細胞に分化誘導し，*in vitro*での疾患モデルの構築や，構築された疾患モデルを利用した創薬プラットフォームの創出が進められている．また，iPS細胞の*in vivo*での活用法としては，ヒト血球抗原（human leukocyte antigen: HLA）ハプロタイプが一致するヒトiPS細胞から分化誘導した細胞を移植する他家移植，または，患者由来の細胞を*in vitro*で治療した細胞を用いた自家移植に関する研究などが進められている．本稿では，iPS細胞を用いた神経疾患研究の現況と今後の課題について述べる．

KEY WORDS
創薬
移植
神経細胞
グリア細胞
モデリング

はじめに

神経変性疾患や精神疾患に関する現在の知見は死後病理組織の解析に基づくものが多い．しかしながら，死後病理組織は疾患の末期での病態を反映し，必ずしも疾患の発症前もしくは進行期での病態を反映するものではない．さらに，死後病理組織は疾患の影響以外に，死後変化などを含め，二次的な影響を受けている可能性がある．一方，原因遺伝子が明らかな疾患では動物モデル・細胞モデルでの解析が進められているが，これらのモデルを用いた治療実験で効果を有した薬剤が臨床試験で必ずしも効果を示すとは限らない[1,2]．

2007年にヒトiPS細胞技術が開発され[3,4]，患者自身の体細胞からiPS細胞を作製し，疾患の標的細胞へ分化させることが可能になった．このことはさらに，患者由来の標的細胞を用いた*in vitro*での疾患モデリング・創薬プラットフォームの開発を可能にしつつある．

また，これまでES細胞や胎児由来細胞が移植細胞のリソースとして使用されてきたが，倫理的・量的制限および拒絶反応が問題であった．しかしながら，iPS細胞技術は移植の新たなツールを提供した．本稿では，神経疾患特異的iPS細胞を用いた疾患モデルの構築・創薬プラットフォームの創出・移植に関する現

1344-0128/11/ ¥100/JCOPY